AGU PUBLICATIONS

Geophysical Research Letters

RESEARCH LETTER
10.1002/2015GL067308

Key Points:
- Marine heatwaves are discrete warming events with an areal extent and duration
- Marine heatwaves are influenced by intrinsic climate variability
- Probability of marine heatwaves is a trade-off between size, intensity, and duration

Supporting Information:
- Texts S1 and S2, Figures S1 and S2, and Table S1

Correspondence to:
H. A. Scannell,
scanh@uw.edu

Citation:
Scannell, H. A., A. J. Pershing, M. A. Alexander, A. C. Thomas, and K. E. Mills (2016), Frequency of marine heatwaves in the North Atlantic and North Pacific since 1950, *Geophys. Res. Lett.*, *43*, 2069–2076, doi:10.1002/2015GL067308.

Received 10 DEC 2015
Accepted 9 FEB 2016
Accepted article online 11 FEB 2016
Published online 3 MAR 2016

Frequency of marine heatwaves in the North Atlantic and North Pacific since 1950

Hillary A. Scannell[1,2], Andrew J. Pershing[2], Michael A. Alexander[3], Andrew C. Thomas[1], and Katherine E. Mills[2]

[1]School of Marine Sciences, University of Maine, Orono, Maine, USA, [2]Gulf of Maine Research Institute, Portland, Maine, USA, [3]NOAA/Earth System Research Laboratory, Boulder, Colorado, USA

Abstract Extreme and large-scale warming events in the ocean have been dubbed marine heatwaves, and these have been documented in both the Northern and Southern Hemispheres. This paper examines the intensity, duration, and frequency of positive sea surface temperature anomalies in the North Atlantic and North Pacific Oceans over the period 1950–2014 using an objective definition for marine heatwaves based on their probability of occurrence. Small-area anomalies occur more frequently than large-area anomalies, and this relationship can be characterized by a power law distribution. The relative frequency of large- versus small-area anomalies, represented by the power law slope parameter, is modulated by basin-scale modes of natural climate variability and anthropogenic warming. Findings suggest that the probability of marine heatwaves is a trade-off between size, intensity, and duration and that region specific variability modulates the frequency of these events.

1. Introduction

Heatwaves on land are becoming more frequent, intense, and persistent due to anthropogenic climate change, and these events have had major impacts on human health and economic productivity [*Meehl and Tebaldi*, 2004; *Stott et al.,* 2004; *Trenberth et al.,* 2007]. A similar phenomenon in the ocean has recently been identified and is associated with adverse consequences to both fishery productivity and marine ecosystems [*Pearce et al.,* 2011; *Mills et al.,* 2013]. These events have been referred to as marine heatwaves and have been described as regions of large-scale and persistent positive sea surface temperature (SST) anomalies [*Pearce et al.,* 2011]. Well-known marine heatwaves have occurred in the Mediterranean Sea [*Black et al.,* 2004; *Olita et al.,* 2007], off Western Australia [*Pearce and Feng*, 2013], in the northwest Atlantic [*Mills et al.,* 2013; *Chen et al.,* 2014, 2015], and in the northeast Pacific [*Bond et al.,* 2015; *Hartmann*, 2015]. Like heatwaves on land, marine heatwaves are likely to become more frequent and intense under continued anthropogenic warming assuming fixed temperature thresholds [*Solomon et al.,* 2007]. However, if temperature fluctuations are examined about the mean warming trend, marine heatwaves occur as spatially and temporally isolated extreme events. This reasoning suggests a level of stochasticity in the likelihood of heatwaves akin to analogous atmospheric phenomena [e.g., *Hunt*, 2007; *Teng et al.,* 2013].

To the first order, stochastic atmospheric forcing modulates the properties of SST anomalies over middle and high latitudes [*Frankignoul and Hasselmann*, 1977]. White-noise variability from the atmosphere produces temperature anomalies in the ocean mixed layer with a redder spectrum (e.g., more variability at larger space and time scales). This view of SST anomalies can be expanded to include stochastic forcing from oceanic flows (e.g., Ekman transport) [*Frankignoul and Reynolds*, 1983]. These stochastic processes, along with phenomena such as El Niño that have deterministic components, interact over time to generate modes of interannual-to-multidecadal variability. The most influential large-scale modes of SST and atmospheric variability in the Northern Hemisphere are the North Atlantic Oscillation (NAO), Atlantic Multidecadal Oscillation (AMO), El Niño–Southern Oscillation (ENSO), and Pacific Decadal Oscillation (PDO). These modes are associated with changes in SSTs at interannual time scales (e.g., NAO and ENSO), as well as at time scales of decades and longer (e.g., AMO and PDO).

Natural oscillations of SST and their associated spatial patterns are well established in the literature [*Wallace and Gutzler*, 1981; *Folland et al.,* 1984; *Mantua et al.,* 1997; *Kerr*, 2000]; however, the variability of marine heatwaves with respect to natural temperature fluctuations have not been explored in a

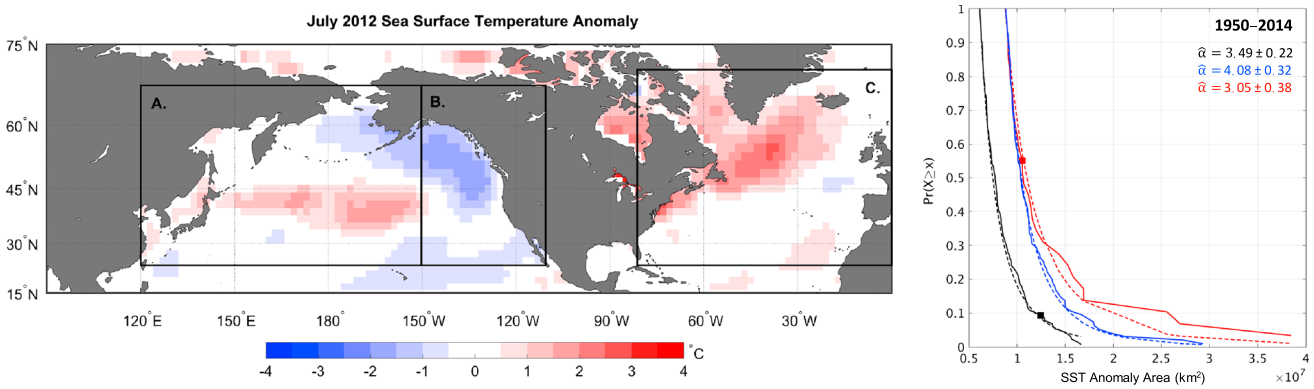

Figure 1. Sea surface temperature anomaly map for July 2012 during the peak of the 2012 northwest Atlantic marine heatwave. Boxes are the regions in the Northern Hemisphere where anomaly data are contoured to find the areal extent of positive SST anomalies and include (a) western North Pacific, (b) eastern North Pacific, and (c) North Atlantic. The complementary cumulative distribution function (CCDF) of the power law distribution is shown for detrended positive SST anomaly areas in the North Atlantic (black), western North Pacific (blue), and eastern North Pacific (red) between 1950 and 2014. The CCDF is defined as 1 minus the integrated probability density function from x to infinity. Solid lines are the empirical CCDF and dashed lines show the theoretical CCDF of the power law. With the long-term trend removed, the 2012 northwest Atlantic marine heatwave is denoted by the black square and the 2013–2014 northeast Pacific marine heatwave by the red square. Derived power law slope parameters (α) and estimated error are color coded for each region as stated above.

historical context. The objectives of this study are to (1) develop a definition for marine heatwaves that is useful in fitting a statistical distribution to the spatial frequency of anomaly areas, (2) examine the trade-offs between intensity and duration in event probability, (3) identify associations between marine heatwave frequency and modes of natural SST variability, and (4) document how the frequency of marine heatwaves has changed with respect to anthropogenic warming. We use 65 years of reconstructed SST data in the Northern Hemisphere where two case study heatwaves have occurred, the 2012 northwest Atlantic [*Mills et al.,* 2013] and 2013–2014 northeast Pacific marine heatwaves [*Bond et al.,* 2015]. These ocean regions are climatically important, as they are influenced by slow-varying modes of intrinsic climate variability [*Deser et al.,* 2010; *Hartmann*, 2015].

2. Data and Methods

We use monthly 2° × 2° resolution gridded SST over the period 1950–2014 from the National Oceanic and Atmospheric Administration's extended reconstructed SST version 3b (ERSSTv3b) data set [*Xue et al.,* 2003; *Smith et al.,* 2008]. Spatial and temporal data sampling in ERSSTv3b has adequate coverage in the North Atlantic and North Pacific regions after 1950 [*Deser et al.,* 2010]. We remove the seasonal cycle and derive anomalies by subtracting the climatological monthly mean at individual grid points. We then compute the least squares fit of SST anomalies between 1950 and 2014 and subtract the linear trend at each grid point. The space domain for the analysis is 20°–70°N in the North Atlantic and 20°–65°N in the North Pacific where the NAO, AMO, and PDO spatial loadings are well defined respectively (see map boxes in Figure 1). The North Pacific study domain is further subdivided at 150°W and is referenced hereafter as the eastern and western North Pacific. This division separates regions that consistently have opposite anomaly signs associated with the loading pattern of the PDO.

Given a map of SST anomalies, we identify discrete warming events by mapping contours (using MATLAB's contour function) of a particular anomaly threshold level. The default threshold is 1 standard deviation (σ) above the regional mean ($\sigma = 0.63$°C western North Pacific, 0.69°C eastern North Pacific, and 0.55°C North Atlantic). This threshold classification emphasizes variability between study regions, and defining anomalies this way creates a data set of anomaly areas for the North Atlantic, eastern North Pacific, and western North Pacific. The distribution of anomaly areas in each region is heavy tailed (Figure 1), meaning that small-area anomalies occur more frequently than large-area anomalies. This suggests that the frequency of the empirical anomaly data, x, may be drawn from the power law distribution,

$$p(x) \propto Cx^{-\alpha}; \tag{1}$$

where α is a scaling parameter and C is a normalizing constant [*Clauset et al.,* 2009]. The rate at which the probability of marine heatwaves decays with increasing area is controlled by α, which we refer to as the slope

of the anomaly size distribution. A large slope ($\alpha = 0.6$) indicates fewer large anomalies occurring; in contrast, a small slope ($\alpha = 0.3$) infers a greater frequency of large-area anomalies. Power laws are commonly used to describe the magnitudes of many physically varying phenomena including earthquakes [*Schorlemmer et al.,* 2005], flood frequencies [*Smith*, 1991], wave heights [*Burroughs and Tebbens*, 2005], solar flares [*Crosby et al.,* 1993], and lunar craters [*Neukum and Ivanov*, 1994]. Describing SST anomalies in this manner provides a meaningful way to characterize the frequency of marine heatwaves [e.g., *Panorska et al.,* 2007].

Phenomena that lead to power law distributions are often most apparent when observations x are greater than some minimum $x_{\min}$ (i.e., toward the heavy side of the distribution). The power law distribution has a normalized probability density $p(x)$ such that,

$$p(x) = \frac{\alpha - 1}{x_{\min}} \left(\frac{x}{x_{\min}} \right)^{-\alpha} \tag{2}$$

[*Newman*, 2005].

We approximate α and $x_{\min}$ in the probability density function equation (2) in order to fit a power law to the distribution of anomaly areas. Assuming some initial arbitrary $x_{\min}$, the method of maximum likelihood estimation (MLE) allows us to approximate a value for α that is most likely to have generated the observed set of anomaly observations above $x_{\min}$. We use the derivation of the MLE under this framework from *Newman* [2005].

When the number of observations is sufficiently large, the MLE α is a good approximation of the true α. However, the approximation for α is only good if we know the value for $x_{\min}$, or in other words, if we know the lower limit for where the power law is obeyed. We obtain an unbiased approximate for $x_{\min}$ using a Kolmogorov-Smirnov (K-S) minimization technique developed by *Clauset et al.* [2009]. This procedure tests every unique data value as a possible $x_{\min}$, truncates the data above this value, and computes the empirical and theoretical complementary cumulative distribution functions (CCDFs). The K-S statistic (D_{KS}) quantifies the maximum distance between the CCDF of the empirical data and the fitted theoretical power law model. We use a Lilliefors corrected K-S test since the parameters of the empirical distribution have been fit using the same data [*Wilks*, 2011]. Lilliefors correction has the same D_{KS} test statistic as the regular K-S test, except the empirical distribution is fit with unknown parameters so that it makes no underlying assumptions about the true distribution (see supporting information). The CCDF is simply one minus the PDF integrated from x to infinity, which gives the exceedance probability such that,

$$P(X \geq x) = 1 - \int_{x}^{\infty} p(x)\mathrm{d}x = 1 - \left(\frac{x}{x_{\min}} \right)^{-\alpha+1}. \tag{3}$$

The CCDF in equation (3) describes the probability of observing an anomaly area X at least as extreme as the x anomaly area observed. Using the likelihood equation and Lilliefors corrected K-S test, we fit a power law distribution to the frequency of anomaly areas using approximated α and $x_{\min}$ parameters. To test whether the power law with the chosen parameters is a good fit to the data, we use the semiparametric bootstrapping technique described in *Clauset et al.* [2009] to generate 2500 sets of synthetic power law data using the fitted α and $x_{\min}$ parameters. With the Lilliefors corrected K-S test again, we measure the distance each synthetic distribution deviates from the true power law model. We use a goodness-of-fit test that generates a p value statistic (P_{KS}) defined by the fraction of simulations where the synthetic D_{KS} is greater or equal to the empirical D_{KS} [*Clauset et al.,* 2009]. If P_{KS} is large or close to 1, this means that the separation between the empirical distribution and the power law model are caused by statistical noise alone and that the model is a good fit to the empirical data. If P_{KS} is ≤ 0.1, there is at most a 1 in 10 probability of fitting a poor model to the data.

We expect that the power law parameters will be sensitive to the SST threshold values used to define an anomaly. We also expect that the frequency of anomalies above a certain size will change with different averaging periods. To examine how the anomaly size distribution changes as a function of intensity (i.e., threshold value) and duration (i.e. averaging period), we develop intensity-duration-frequency (IDF) plots for each region. IDF plots are a technique originally used by hydrologists for summarizing rainfall event probabilities [*Chow et al.*, 1988; *Koutsoyiannis et al.,* 1998]. We develop IDF plots by computing a single slope parameter α from all monthly SST anomaly areas between the period 1950 and 2014 using various temperature thresholds (intensity) and averaging intervals (duration). This produces a matrix of power law slope values for each intensity-duration combination. The slope values are used in the CCDF equation (3) to solve for the

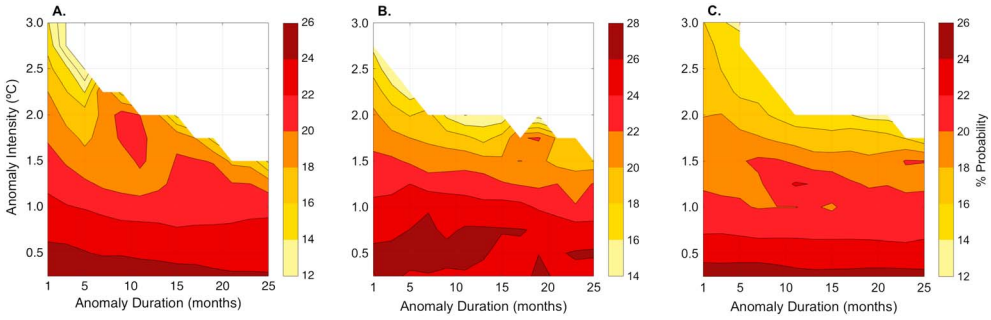

Figure 2. Intensity, duration, and frequency as percent probability for a 7.60×10^6 km^2 or larger anomaly (25% of the North Atlantic study area) in the (a) western North Pacific, (b) eastern North Pacific, and (c) North Atlantic defined by solid black boxes in Figure 1. The probability is given by the complementary cumulative distribution of anomaly areas with a calculated slope based on the detrended 1950–2014 set of positive SST observations. Red colors indicate events that are more probable than yellow.

probability of observing an anomaly with an areal extent of 7.60×10^6 km^2 or larger (25% of the North Atlantic or western North Pacific study area). This magnitude of anomaly area is on the order of the 2012 northwest Atlantic and 2013–2014 northeast Pacific marine heatwaves. The resulting probability outcomes are summarized as IDF contours (i.e., lines of constant probability).

The slope of the power law distribution can also be derived from the subset of anomalies co-occurring with the positive and negative phases of the PDO, ENSO, AMO, and NAO. Positive and negative phases are defined as the upper and lower third of the climate indices. We calculate the power law slope parameter by fitting the distribution to the subset of anomalies corresponding to the positive and negative phases of climate indices in each region.

3. Results

The areal extent of SST anomalies follows a power law distribution in the North Atlantic and North Pacific, and the empirical distribution of anomaly data resembles the theoretical power law model (Figure 1). The P_{KS} statistic of the goodness-of-fit test is greater than 0.1 in all three regions ($P_{KS} = 0.95$ western North Pacific, 0.79 eastern North Pacific, and 0.22 North Atlantic), which supports the hypothesis that these data come from a power law distribution. Differences in the CCDFs between regions suggest that the power law parameters may vary by location. The North Atlantic power law distribution of detrended SST anomalies has a smaller minimum area ($x_{min} = 6.13 \times 10^6$ km^2) compared to both the eastern and western North Pacific regions, while the western North Pacific has the largest minimum area in the anomaly power law distribution ($x_{min} = 8.82 \times 10^6$ km^2). The two North Pacific CCDFs are both constrained by relatively large anomaly areas of similar magnitude. This suggests that the power law distribution in these regions experience larger anomalies than in the North Atlantic. This is not likely due to the overall size of each region, as the North Atlantic is larger comparatively. Instead, it may be related to the underlying physical drivers of the distribution.

Two well-documented marine heatwaves occurred in the Northern Hemisphere within the past 4 years: the 2012 event in the northwest Atlantic and the 2013–2014 event in the eastern North Pacific. The 2012 northwest Atlantic marine heatwave was at least 1.10°C above the 1950–2014 climatology, had an areal extent of 7.60×10^6 km^2, and persisted for 3 months (June–August 2012). Smaller regions in the northwest Atlantic during this event had SST anomalies exceeding 3°C (5.5 standard deviations). Comparatively, the 2013–2014 eastern North Pacific marine heatwave developed in August 2013 and persisted through December 2014. The maximum areal extent of this event was on the order of 9.09×10^6 km^2. During January 2014 this event had a mean SST anomaly of 1.5°C and a local maximum of 2.8°C. The Pacific anomaly was spatially larger and lasted longer than the Atlantic heatwave, but it was less intense.

To understand how temperature covaries with the duration of marine heatwaves, we use intensity-duration-frequency (IDF) relationships for a 7.60×10^6 km^2 or larger marine heatwave (>25% of the North Atlantic study area). The overall pattern of the IDF plots is similar between regions, with probability diminishing rapidly with temperature intensity and gradually with anomaly duration (Figure 2). In general, the probability

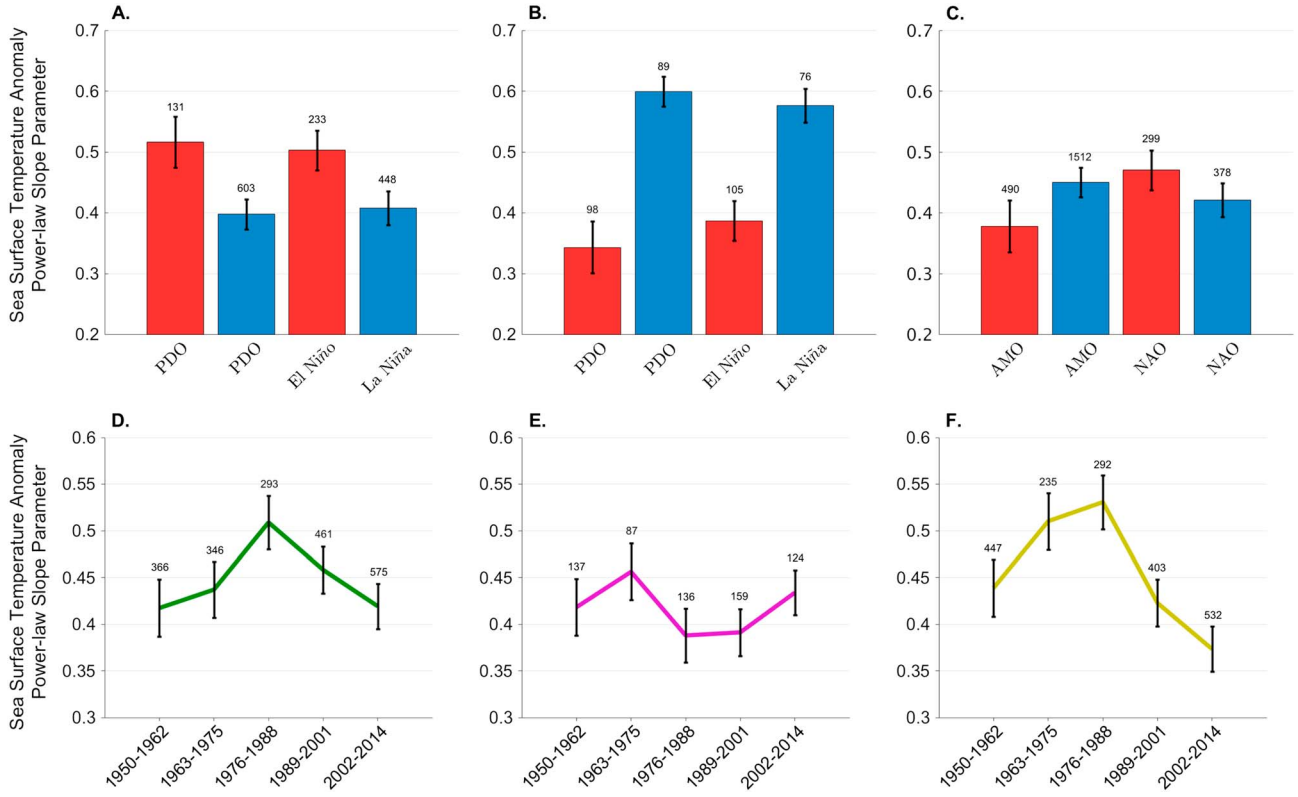

Figure 3. Power law parameters used to infer the anomaly size frequency of positive detrended monthly anomalies between 1950–2014 in the (a) western North Pacific, (b) eastern North Pacific, and (c) North Atlantic during positive (red) and negative (blue) phases of intrinsic climate modes. (d–f) The power law parameter for positive sea surface temperature anomalies referenced to the 1950–2014 long-term warming trend in the (Figure 3d) western North Pacific, (Figure 3e) eastern North Pacific, and (Figure 3f) North Atlantic for sequential 13 year periods. Error bars represent calculated standard error, and the number of observations in the tail of the power law is displayed above each error bar.

of marine heatwaves is highest (26–28%) for low-intensity thresholds (0.5°C) and short-lived events (<5 months). As the intensity of an event increases, the probability declines, falling to less than 14% for a 3°C anomaly. According to this analysis, a 3°C marine heatwave persisting for longer than 5 months has not been observed since at least 1950.

In general, probability declines with increasing duration; however, there is an exception that occurs in the western North Pacific centered around 9 to 11 months and 1.4 to 2.1°C (Figure 2a). This feature appears as a node of increased probability surrounded by lower probability and is consistent with the reemergence hypothesis of SST anomalies [*Alexander et al.,* 1999]. This hypothesis states that winter SST anomalies stored within the seasonal thermocline during the summer reappear the following winter. The IDF curves suggest that SST reemergence may be an important component in the frequency of marine heatwaves on annual-to-interannual time scales and is most pronounced in the western North Pacific (See Text S2 and Figure S2 in the supporting information for further discussion).

Based on the IDF analysis, heatwave events with the intensity and duration of the 2012 northwest Atlantic heatwave (1.10°C and 3 months) have less than a 20% probability of occurring in the North Atlantic, 24% in the eastern North Pacific, and 20% in the western North Pacific (Figure 2). These statistics imply that marine heatwaves of this magnitude should naturally occur approximately once every 5 years or less.

SST anomalies are often connected through intrinsic modes of SST variability in each basin. We expect that these variations would alter the frequency distribution of positive SST anomaly areas. The slope of the power law distribution in the eastern North Pacific is small ($\alpha = 0.34$) during the positive phase of the PDO and large ($\alpha = 0.60$) during the negative phase. In the western North Pacific, the positive phase of the PDO coincides with a large power law slope ($\alpha = 0.52$), and the negative phase of the PDO is associated with a small power law slope ($\alpha = 0.40$) (Figures 3a and 3b). The power law distribution of anomaly area flattens when the slope is

small and increases the probability of a large area positive SST anomaly that is characteristic of a marine heatwave. On interannual time scales, the PDO can be described as a long-lived ENSO-like pattern of SST variability that alternates between warm and cold states. The dipole Pacific SST response to alternating El Niño and La Niña states is also noticeable from changes in the power law slope (Figures 3a and 3b). During El Niño, the eastern North Pacific has a greater frequency of marine heatwaves ($\alpha = 0.38$) compared to the western North Pacific ($\alpha = 0.50$). This relationship is reversed for La Niña events where the western North Pacific has a greater frequency of marine heatwaves ($\alpha = 0.40$) than the eastern North Pacific ($\alpha = 0.58$).

Similar relationships between intrinsic climate modes and the frequency of marine heatwaves can be diagnosed in the North Atlantic. Here the size-frequency distribution of positive SST anomalies changes with respect to the AMO and NAO. The power law distribution flattens during the positive phase of the AMO ($\alpha = 0.37$) when basin-wide temperatures are warmer than average. During the cool phase of the AMO the distribution of anomalies tightens ($\alpha = 0.45$), and large positive SST anomalies are less prevalent. Variability in the anomaly size distribution during phase changes of the NAO is not as pronounced. Small changes in the power law slope during the negative NAO phase are associated with frequent large positive SST anomalies ($\alpha = 0.42$) compared to the positive NAO phase ($\alpha = 0.46$). The AMO is more dominate than the NAO in modulating the size frequency of positive SST anomalies in the North Atlantic; however, the superimposed contributions of both phenomena may play an important role in influencing marine heatwave probability.

Our analysis was conducted on detrended data, effectively removing the signal of anthropogenic warming. Defining anomalies this way is appropriate for examining the underlying probability distribution; however, absolute temperatures have significant impacts on ecological conditions. If anomalies are defined relative to a fixed monthly long-term average and contoured above 1 standard deviation for each region, we expect that large area positive anomalies will occur more frequently in the 21st century. This relationship is complicated, perhaps due to the persistent memory and large heat capacity of the ocean. The slope of the power law distribution for positive SST anomaly areas is computed for each 13 year period between 1950 and 2014 (Figures 3d–3f). The spread of the distribution slopes range from $\alpha = 0.37$ to 0.51. Recall that $\alpha = 0.37$ suggests that large-area positive anomalies are more frequent than a distribution with $\alpha = 0.51$. During 1976–1998, the eastern North Pacific has a slope value much less than the western North Pacific and Atlantic. This is likely due to the 1982–1983 El Niño. Similarly, for the period 1989–2001, the anomalous 1997–1998 El Niño likely influenced the occurrence of very large anomalies in the eastern North Pacific, a relationship previous described in Figures 3a and 3b. A possible decline in α is most noticeable after 1976 in the North Atlantic and western North Pacific (Figures 3d and 3f), coincident with when the rate of mean global warming began to accelerate [*Meehl et al.,* 2009].

4. Conclusion

We show that the frequency of marine heatwaves is a trade-off between size, intensity, and duration, and this can be best described by a power law distribution. Not surprisingly, small-area anomalies occur more frequently than large-area anomalies, and this is likely due to the dampening effects of the atmosphere and ocean mixing processes. If we define a marine heatwave similar to the 2012 northwest Atlantic event (3 months, 7.60×10^6 km^2 and 1.10°C (2σ) above the 1950–2014 climatology), then we can quantify the statistical properties of these events. We find that marine heatwaves have a probability of 20% in the western North Pacific, 24% in the eastern North Pacific, and 20% in the North Atlantic. These statistics imply that marine heatwaves on par with the 2012 northwest Atlantic event should naturally occur once every 5 years or less. However, the intensity and duration of marine heatwaves are also modulated by modes of intrinsic climate variability that oscillate on interannual-to-multidecadal time scales.

In the North Pacific the PDO is the leading mode of SST variability with anomalies of opposite sign in the central-western North Pacific compared to those in the east [*Mantua et al.,* 1997]. The PDO dominates the size variability of SST anomalies in the North Pacific and its east-west dipole structure in SST pattern increases marine heatwave probability during the positive phase in the eastern North Pacific and during the negative phase in the western North Pacific. The PDO is not necessarily a distinct phenomenon but rather influenced in the eastern Pacific by an extratropical atmospheric response due to ENSO (e.g., atmospheric bridge) [*Alexander et al.,* 2002]. Consistent with this linkage, we find that ENSO has a dominant influence on marine heatwaves in the eastern North Pacific during El Niño and in the western North Pacific during La Niña.

In the North Atlantic, the AMO is a coherent large-scale pattern of SST variability with a nonrandom multidecadal time scale [*Folland et al.,* 1984; *Kushnir*, 1994; *Schlesinger and Ramankutty*, 1994; *Kerr*, 2000]. The AMO has been in a positive phase since the middle 1990s and is associated with positive SST anomalies in the North Atlantic [*Deser et al.,* 2010]. Persistent SST patterns in the North Atlantic are also associated with the NAO and have been well documented [*Czaja and Frankignoul*, 2002; *Marshall et al.,* 2001; *Visbeck et al.,* 2003]. Weak anomalies in SST generated by the NAO are induced via atmospheric forcing on monthly and seasonal time scales through air-sea heat fluxes and wind-driven Ekman transport [*Battisti et al.,* 1995; *Deser and Timlin*, 1997; *Hurrell and Deser*, 2009]. Prolonged negative NAO forcing may induce basin-wide SST anomalies and increase the likelihood of marine heatwaves occurring. The NAO is not significantly correlated with the AMO, and we show that the AMO is the dominant modulator of Atlantic SSTs. The 2012 northwest Atlantic marine heatwave began with strong positive NAO conditions in late 2011 [*Chen et al.,* 2014]. Positive AMO conditions persisted throughout the year, likely increasing the likelihood of a marine heatwave in the northwest Atlantic during 2012.

We have demonstrated that the size variance of extratropical positive SST anomalies can be well represented by the power law distribution. On interannual-to-multidecadal time scales, intrinsic climate variability influences the size-frequency patterns of marine heatwaves in the North Atlantic and North Pacific. When the long-term warming trend is removed from SSTs, random weather-like processes that change ocean temperatures within the mixed layer influence the size-frequency of marine heatwaves over time. This emphasizes the unpredictable nature of marine heatwaves, which makes them intrinsically difficult to forecast with significant lead-time. Unlike marine heatwaves, modes of natural SST variability have been well studied, and our ability to forecast these oscillations has become more skillful [e.g., *Mochizuki et al.,* 2010; *Kim et al.,* 2012]. Understanding the natural drivers of marine heatwaves may increase our ability to assess the likelihood of these events occurring in the future, when long-term warming will become more conducive to more frequent and longer-lasting events.

The spatial and temporal scales of marine heatwaves are significant sources of variability in the ocean and are newly emerging areas of research. Power laws are commonly used to describe many natural extreme phenomena, and we have tested and applied these concepts to SST anomalies.

Acknowledgments

The NSF Coastal SEES grant OCE1325484 supported this research. The ERSSTv3b was provided by NOAA/NCDC. NOAA/PSD provided the AMO unsmoothed 1948 to present and Nino3.4 indices. The NAO index was provided by NOAA/CPC, and the PDO index was from Nathan Mantua at the University of Washington (http://research.jisao.washington.edu/pdo/PDO.latest). We are grateful for two anonymous reviewers for their help in improving this manuscript and discussions with Patrick Sullivan of Cornell University.

References

Alexander, M. A., C. Deser, and M. S. Timlin (1999), The reemergence of SST anomalies in the North Pacific Ocean, *J. Clim.*, *12*(8), 2419–2433, doi:10.1175/1520-0442(1999)012<2419:TROSAI>2.0.CO;2.

Alexander, M. A., I. Bladé, M. Newman, J. R. Lanzante, N.-C. Lau, and J. D. Scott (2002), The atmospheric bridge: the influence of ENSO teleconnections on air-sea interaction over the global oceans, *J. Clim.*, *15*(16), 2205–2231, doi:10.1175/1520-0442(2002)015<2205:TABTIO>2.0.CO;2.

Battisti, D. S., U. S. Bhatt, and M. A. Alexander (1995), A modeling study of the interannual variability in the wintertime North Atlantic Ocean, *J. Clim.*, *8*(12), 3067–3083, doi:10.1175/1520-0442(1995)008<3067:AMSOTI>2.0.CO;2.

Black, E., M. Blackburn, G. Harrison, B. Hoskins, and J. Methven (2004), Factors contributing to the summer 2003 European heatwave, *R. Meteorol. Soc. Weather*, *59*(8), 217–223, doi:10.1256/wea.74.04.

Bond, N. A., M. F. Cronin, H. Freeland, and N. Mantua (2015), Causes and impacts of the 2014 warm anomaly in the NE Pacific, *Geophys. Res. Lett.*, *42*, 3414–3420, doi:10.1002/2015GL063306.

Burroughs, S. M., and S. F. Tebbens (2005), Power-law scaling and probabilistic forecasting of tsunami runup heights, *Pure Appl. Geophys.*, *162*, 331–343.

Chen, K., G. G. Gawarkiewicz, S. J. Lentz, and J. M. Bane (2014), Diagnosing the warming of the Northeastern U.S. Coastal Ocean in 2012: A linkage between the atmospheric jet stream variability and ocean response, *J. Geophys. Res. Oceans*, *119*, 218–227, doi:10.1002/2013JC009393.

Chen, K., G. Gawarkiewicz, Y.-O. Kwon, and W. G. Zhang (2015), The role of atmospheric forcing versus ocean advection during the extreme warming of the Northeast U.S. continental shelf in 2012, *J. Geophys. Res. Oceans*, *120*, 4324–4339, doi:10.1002/2014JC010547.

Chow, V. T., D. R. Maidment, and L. W. Mays (1988), *Applied Hydrology*, McGraw-Hill, New York.

Clauset, A., C. R. Shalizi, and M. E. J. Newman (2009), Power-law distributions in empirical data, *SIAM Rev.*, *51*(4), 661–703, doi:10.1137/070710111.

Crosby, N. B., M. J. Aschwanden, and B. R. Dennis (1993), Frequency distributions and correlations of solar X-ray flare parameters, *Sol. Phys.*, *143*(2), 275–299, doi:10.1007/BF00646488.

Czaja, A., and C. Frankignoul (2002), Observed impact of Atlantic SST anomalies on the North Atlantic Oscillation, *J. Clim.*, *15*(6), 606–623, doi:10.1175/1520-0442(2002)015<0606:OIOASA>2.0.CO;2.

Deser, C., and M. S. Timlin (1997), Atmosphere-ocean interaction on weekly time scales in the North Atlantic and Pacific, *J. Clim.*, *10*(3), 393–408, doi:10.1175/1520-0442(1997)010<0393:AOIOWT>2.0.CO;2.

Deser, C., M. A. Alexander, S.-P. Xie, and A. S. Phillips (2010), Sea surface temperature variability: Patterns and mechanisms, *Annu. Rev. Mar. Sci.*, *2*, 115–143, doi:10.1146/annurev-marine-120408-151453.

Folland, C. K., D. E. Parker, and F. E. Kates (1984), Worldwide marine temperature fluctuations. 1856–1981, *Nature*, *310*, 670–673, doi:10.1038/310670a0.

Frankignoul, C., and K. Hasselmann (1977), Stochastic climate models, Part II Application to sea-surface temperature anomalies and thermocline variability, *Tellus*, *29*(4), 289–305, doi:10.1111/j.2153-3490.1977.tb00740.x.

Frankignoul, C., and R. W. Reynolds (1983), Testing a dynamical model for mid-latitude surface temperature anomalies, *J. Phys. Oceanogr.*, *13*(7), 1131–1145, doi:10.1175/1520-0485(1983)013<1131:TADMFM>2.0.CO;2.

Hartmann, D. L. (2015), Pacific sea surface temperature and the winter of 2014, *Geophy. Res. Lett.*, *42*, 1894–1902, doi:10.1002/2015GL063083.

Hunt, B. G. (2007), A climatology of heat waves from a multimillennial simulation, *J. Clim.*, *20*(15), 3802–3821, doi:10.1175/JCLI4224.1.

Hurrell, J. W., and C. Deser (2009), North Atlantic climate variability: The role of the North Atlantic Oscillation, *J. Mar. Syst.*, *78*(1), 28–41, doi:10.1016/j.jmarsys.2008.11.026.

Kim, H.-M., P. J. Webster, and J. A. Curry (2012), Evaluation of short-term climate change prediction in multi-model CMIP5 decadal hindcasts, *Geophys. Res. Lett.*, *39*, L10701, doi:10.1029/2012GL051644.

Kerr, R. A. (2000), A North Atlantic climate pacemaker for centuries, *Science*, *288*, 1984–1985, doi:10.1126/science.288.5473.1984.

Koutsoyiannis, D., D. Kozonis, and A. Manetas (1998), A mathematical framework for studying rainfall intensity-duration-frequency relationships, *J. Hydrol.*, *206*(1–2), 118–135, doi:10.1016/S0022-1694(98)00097-3.

Kushnir, Y. (1994), Interdecadal variations in North Atlantic sea surface temperature and associated atmospheric conditions, *J. Clim.*, *7*, 141–157, doi:10.1175/1520-0442(1994)007<0141:IVINAS>2.0.CO;2.

Mantua, N. J., S. R. Hare, Y. Zhang, J. M. Wallace, and R. C. Francis (1997), A pacific interdecadal climate oscillation with impacts on salmon production, *Bull. Am. Meteorol. Soc.*, *78*(6), 1069–1079, doi:10.1175/1520-0477(1997)078<1069:APICOW>2.0.CO;2.

Marshall, J., Y. Kushnir, D. Battisti, P. Chang, A. Czaja, R. Dickson, J. Hurrell, M. McCartney, R. Saravanan, and M. Visbeck (2001), North Atlantic climate variability, phenomena, impacts and mechanisms, *Int. J. Climatol.*, *21*(15), 1863–1898, doi:10.1002/joc.693.

Meehl, G. A., and C. Tebaldi (2004), More intense, more frequent, and longer lasting heat waves in the 21st century, *Science*, *305*, 994–997, doi:10.1002/joc.693.

Meehl, G. A., A. Hu, and B. D. Santer (2009), The mid-1970s climate shift in the Pacific and relative roles of forced versus inherent decadal variability, *J. Clim.*, *22*, 780–792, doi:10.1175/2008JCLI2552.1.

Mills, K. E., et al. (2013), Fisheries management in a changing climate: Lessons from the 2012 ocean heat wave in the Northwest Atlantic, *Oceanography*, *26*(2), 191–195, doi:10.5670/oceanog.2013.27.

Mochizuki, T., et al. (2010), Pacific decadal oscillation hindcasts relevant to near-term climate prediction, *Proc. Natl. Acad. Sci. U.S.A.*, *107*(5), 1833–1837, doi:10.1073/pnas.0906531107.

Neukum, G., and B. A. Ivanov (1994), Crater size distributions and impact probabilities on Earth from lunar, terrestrial-planet, and asteroid cratering data, in *Hazards Due to Comets and Asteroids*, edited by T. Gehrels, pp. 359–416, Univ. of Arizona Press, Tucson.

Newman, M. E. (2005), Power laws, Pareto distributions and Zipf's law, *Contemp. Phys.*, *46*, 323–352, doi:10.1080/00107510500052444.

Olita, A., R. Sorgente, S. Natale, S. Gabersek, A. Ribotti, A. Bonanno, and B. Patti (2007), Effects of the 2003 European heatwave on the Central Mediterranean Sea: Surface fluxes and the dynamical response, *Ocean Sci.*, *3*(2), 273–289, doi:10.5194/os-3-273-2007.

Panorska, A. K., A. Gershunov, and T. J. Kozubowski (2007), From diversity to volatility: Probability of daily precipitation extremes, in *Nonlinear Dynamics in Geosciences*, edited by A. Tsonis and J. Elsner, pp. 465–484, Springer, New York, doi:10.1007/978-0-387-34918-3_26.

Pearce, A., R. Lenanton, G. Jackson, J. Moore, M. Feng, and D. Gaughan (2011), The "marine heat wave" off Western Australia during the summer of 2010/11, Fisheries Research Report No. 222, Department of Fisheries, Western Australia. 40 pp.

Pearce, A. F., and M. Feng (2013), The rise and fall of the "marine heat wave" off Western Australia during the summer of 2010/2011, *J. Mar. Syst.*, *111–112*, 139–156, doi:10.1016/j.jmarsys.2012.10.009.

Schlesinger, M. E., and N. Ramankutty (1994), An oscillation in the global climate system of period 65–70 years, *Nature*, *367*, 723–726, doi:10.1038/367723a0.

Schorlemmer, D., S. Wiemer, and M. Wyss (2005), Variations in earthquake-size distribution across different stress regimes, *Nature*, *437*, 539–542, doi:10.1038/nature04094.

Smith, J. A. (1991), Estimating the upper tail of flood frequency distributions, *Water Resour. Res.*, *23*(8), 1657–1666, doi:10.1029/WR023i008p01657.

Smith, T. M., R. W. Reynolds, T. C. Peterson, and J. Lawrimore (2008), Improvements to NOAA's historical merged land-ocean surface temperature analysis (1880–2006), *J. Clim.*, *21*, 2283–2296, doi:10.1175/2007JCLI2100.1.

Solomon, S., D. Qin, M. Manning, Z. Chen, M. Marquis, K. B. Averyt, M. Tignor, and H. L. Miller (2007), *Contribution of Working Group 1 to the Fourth Assessment Report of the IPCC*, Cambridge Univ. Press, Cambridge, U. K., and New York.

Stott, P. A., D. A. Stone, and M. R. Allen (2004), Human contribution to the European heatwave of 2003, *Nature*, *432*, 610–614, doi:10.1038/nature03089.

Teng, H., G. Branstator, H. Wang, G. A. Meehl, and W. M. Washington (2013), Probability of US heat waves affected by a subseasonal planetary wave pattern, *Nat. Geosci.*, *6*, 1056–1061, doi:10.1038/ngeo1988.

Trenberth, K. E., et al. (2007), Observations: Surface and atmospheric climate change, in *Climate Change 2007: The Physical Science Basis. Contribution of Working Group I to the Fourth Assessment Report of the Intergovernmental Panel on Climate Change*, edited by S. Solomon et al., Cambridge Univ. Press, Cambridge, U. K., and New York.

Visbeck, M., E. P. Chassignet, R. G. Curry, T. L. Delworth, R. R. Dickson, and G. Krahmann (2003), The ocean's response to North Atlantic Oscillation variability, in *The North Atlantic Oscillation, Climatic Significance and Environmental Impact*, *Geophys. Monogr. Ser.*, vol. 134, edited by J. W. Hurrell et al., pp. 113–146, AGU, Washington, D. C., doi:10.1029/134GM06.

Wallace, J. M., and D. S. Gutzler (1981), Teleconnections in the geopotential height field during the northern hemisphere winter, *Mon. Weather Rev.*, *109*, 784–812, doi:10.1175/1520-0493(1981)109<0784:TITGHF>2.0.CO;2.

Wilks, D. S. (2011), *Statistical Methods in the Atmospheric Sciences*, 3rd ed., Elsevier, Amsterdam.

Xue, Y., T. M. Smith, and R. W. Reynolds (2003), Interdecadal changes of 30-yr SST normals during 1871–2000, *J. Clim.*, *16*(10), 1601–1612, doi:10.1175/1520-0442-16.10.160.